First measurement of the $B(E2; 3/2^- \rightarrow 1/2^-)$ transition strength in ^{7}Be: Testing *ab initio* predictions for $A = 7$ nuclei

S. L. Henderson,[1] T. Ahn,[1,*] M. A. Caprio,[2] P. J. Fasano,[2] A. Simon,[1] W. Tan,[1] P. O'Malley,[1] J. Allen,[1] D. W. Bardayan,[1] D. Blankstein,[1] B. Frentz,[1] M. R. Hall,[1] J. J. Kolata,[1] A. E. McCoy,[2,3] S. Moylan,[1] C. S. Reingold,[1] S. Y. Strauss,[1] and R. O. Torres-Isea[4]

[1]*Department of Physics and the Joint Institute for Nuclear Astrophysics, University of Notre Dame, 225 Nieuwland Science Hall, Notre Dame, Indiana 46556, USA*

[2]*Department of Physics, University of Notre Dame, 225 Nieuwland Science Hall, Notre Dame, Indiana 46556, USA*

[3]*TRIUMF, Vancouver, British Columbia V6T 2A3, Canada*

[4]*Department of Physics, Randall Lab, 450 Church Street, University of Michigan, Ann Arbor, Michigan 48109, USA*

(Received 5 February 2019; published 18 June 2019)

Electromagnetic observables are able to give insight into collective and emergent features in nuclei, including nuclear clustering. These observables also provide strong constraints for *ab initio* theory, but comparison of these observables between theory and experiment can be difficult due to the lack of convergence for relevant calculated values, such as $E2$ transition strengths. By comparing the ratios of $E2$ transition strengths for mirror transitions, we find that a wide range of *ab initio* calculations give robust and consistent predictions for this ratio. To experimentally test the validity of these *ab initio* predictions, we performed a Coulomb excitation experiment to measure the $B(E2; 3/2^- \rightarrow 1/2^-)$ transition strength in ^{7}Be for the first time. A $B(E2; 3/2^- \rightarrow 1/2^-)$ value of $26(6)_{\text{stat}}(3)_{\text{syst}}\ e^2\text{fm}^4$ was deduced from the measured Coulomb excitation cross section. This result is used with the experimentally known ^{7}Li $B(E2; 3/2^- \rightarrow 1/2^-)$ value to provide an experimental ratio to compare with the *ab initio* predictions. Our experimental value is consistent with the theoretical ratios within 1σ uncertainty, giving experimental support for the value of these ratios. Further work in both theory and experiment can give insight into the robustness of these ratios and their physical meaning.

DOI: 10.1103/PhysRevC.99.064320

I. INTRODUCTION

Electromagnetic observables are sensitive probes of nuclear structure and have sometimes yielded surprising and important results. For example, in heavy nuclei, the discovery of nuclear deformation [1] and later superdeformation [2], both major advances in our understanding of nuclear structure, have come from detailed studies of electromagnetic transition strengths. The importance of electromagnetic probes and observables extend outside of low-energy nuclear physics. For example, the use of high-energy electron scattering has led to the elucidation of the charge distribution of the neutron [3,4] and the discovery of the EMC effect [5,6], and continues to play a role in solving the proton radius puzzle [7]. In light nuclei, the magnitude of electromagnetic transition strengths can point to the existence of cluster states, halo nuclei, or changes in nuclear deformation. For example, clustering enhances the $E2$ transition strength, due to clustered states having large deformation.

In addition, electromagnetic observables can provide a stringent test of *ab initio* nuclear theory. For instance, several electromagnetic transition strengths have been determined to high precision in $A = 10$ nuclei using lifetime and branching ratio measurements and then compared to *ab initio* quantum Monte Carlo calculations [8–11]. It was found that the calculated $E2$ transition strengths were sensitive to the three-body interaction used. However, regardless of the three-body interaction, the calculations could not consistently reproduce the $E2$ transition strengths across the $A = 10$ isobars, raising questions about the sufficiency of the interactions used [9].

Ab initio nuclear theory attempts to predict the properties of nuclei starting directly from the description of the nucleus in terms of nucleons and their interactions [12–18]. The ingredients which comprise this formulation of the problem are well-defined: once it is assumed that the nucleus can be treated as a system of nucleons described by the nonrelativistic Schrödinger equation, then the energies and wave functions of the nuclear eigenstates depend only on the internucleon interaction [19], which is the input to the *ab initio* theory. However, the internucleon interaction is imperfectly known. It can only be partially determined from nucleon-nucleon scattering data. Modern chiral effective field theory (χEFT) techniques aim to resolve the ambiguities in the interaction by obtaining a systematic series expansion, in which only a handful of low-energy constants remain to be determined from other experimental inputs (such as pion-nucleon scattering or bound-state properties of the $A = 2$ and 3 few-body systems [20]). Precision tests of the *ab initio* predictions will be crucial in validating the resulting χEFT description of nuclei.

An experimental test of *ab initio* predictions, at least in principle, directly tests the validity of the *ab initio* framework

*tan.ahn@nd.edu

and the inputs entering into the *ab initio* picture of the nucleus. However, to get from the *ab initio* formulation of the nuclear problem to concrete *ab initio* predictions for nuclear observables, we must overcome the formidable practical challenge of obtaining accurate numerical solutions to the many-body Schrödinger equation for the A-body system of interacting nucleons. While several approaches have been developed for solving the *ab initio* nuclear many-body problem, including quantum Monte Carlo (QMC) methods [13,21] and the no-core shell model (NCSM) [12,22,23] and its extensions [24–28], each method is constrained by available computational resources. Only truncated calculations of finite numerical accuracy can be carried out. The computed observables, such as electromagnetic transition strengths, must be obtained with sufficient accuracy to allow for meaningful comparison with experiment.

Although $E2$ transition strengths are observables of special interest due to their sensitivity to nuclear shapes and deformation, the $E2$ operator is also sensitive to the large distance "tails" of the nuclear wave function. It is therefore especially challenging to obtain numerically converged *ab initio* calculations of $E2$ strengths [29,30]. Inadequate convergence precludes meaningful comparison of the calculated $E2$ strengths with experiment, at least on an *individual* basis.

However, we find that the *ratios* of calculated $E2$ strengths for pairs of transitions can indeed be well-converged, allowing for direct and meaningful comparison with experiment. This is particularly true where the transitions being compared involve states for which the wave functions all have similar convergence properties. Notably, the wave functions for isospin mirror states are closely related, making the comparison of $E2$ transitions in mirror nuclei a particularly favorable case for obtaining precision tests of *ab initio* theory.

The $B(E2; 3/2^- \rightarrow 1/2^-)$ transitions in the $A = 7$ mirror nuclei ^{7}Li and ^{7}Be therefore provide a natural opportunity for testing *ab initio* theory. While the $B(E2; 3/2^- \rightarrow 1/2^-)$ ground state $E2$ transition strength in ^{7}Li is known from a number of Coulomb excitation experiments [31], the corresponding $E2$ transition strength in ^{7}Be has never been measured. Since the decay of the $1/2^-$ excited state to the $3/2^-$ ground state is predominantly $M1$ in character, the known lifetime of the $1/2^-$ level [32,33] only provides information on the $M1$ transition strength. In contrast, Coulomb excitation provides a viable mechanism for obtaining the $E2$ strength.

To measure the $B(E2; 3/2^- \rightarrow 1/2^-)$ transition strength in ^{7}Be, we have performed a Coulomb-excitation experiment using a radioactive beam of ^{7}Be. The measurement of this transition strength provides a rare test for the $E2$ predictions of a large range of *ab initio* calculations [34–38], involving a variety of traditional and chiral internucleon interactions [20,39–44], and including new NCSM calculations presented here.

II. EXPERIMENT

The Coulomb excitation experiment was performed using a radioactive beam of ^{7}Be at the Nuclear Science Laboratory (NSL) located at the University of Notre Dame. The NSL FN Tandem Van de Graaff accelerator was used to accelerate a

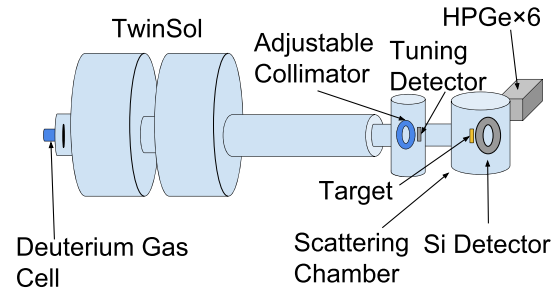

FIG. 1. A drawing showing the different components of the beamline, including Si and HPGe detectors, adjustable collimator, tuning detector, and Au target foil. Drawing is not to scale.

1.5-$e\mu$A primary beam of ^{6}Li to 34.0 MeV. By impinging the beam onto a ^{2}H gas cell at 800 Torr, we produced ^{7}Be through the ^{6}Li(^{2}H, n)^{7}Be reaction. The secondary ^{7}Be beam had an energy of 31.3(10) MeV and was collected and separated from competing reaction products using the two superconducting solenoid magnets of *TwinSol* [45]. A diagram of the *TwinSol* beamline is shown in Fig. 1. The first solenoid was set at 1.9 T and the second at 1.3 T to minimize the level of contaminants in the beam by focusing the beam through a 10-mm-diameter collimator at the crossover position between solenoids, seen in Fig. 2. More details on using *TwinSol* for γ-ray spectroscopy and Coulomb excitation can be found in Refs. [46–48].

Downstream from *TwinSol*, the beam was focused through an adjustable collimator set to a 9-mm radius and then into the scattering chamber 35 cm downstream from the collimator. The ^{7}Be beam was initially tuned through the collimator onto a Si surface barrier detector on a ladder directly after the collimator, then through an empty frame at the target location. This Si tuning detector showed 85% of the beam to be ^{7}Be with ^{6}Li and ^{7}Li comprising the majority of the beam contaminants along with small amounts of ^{4}He. Both contaminants had lower energies than the ^{7}Be ions and could be separated in energy.

Inside the target chamber, the beam scattered off a 1-μm-thick Au foil. We selected Au for its high Z and the energy was chosen to be 77% of the Coulomb barrier to eliminate any

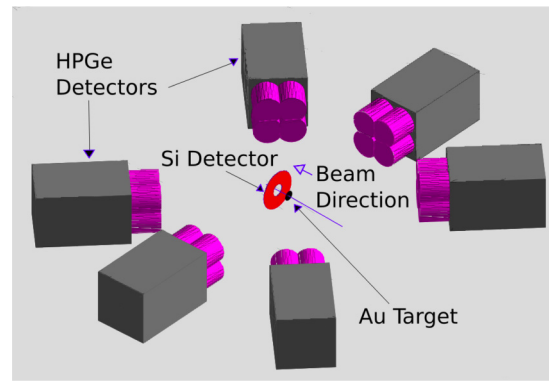

FIG. 2. The experimental setup is shown. Six HPGe Clover detectors placed at 45°, 90°, and 135° with respect to the beam axis are shown surrounding the Au target and S2 Si detector.

significant contribution from the nuclear interaction. A 300-μm-thick Micron Semiconductor Limited S2 annular Si detector was placed 25 mm downstream from the foil to measure the position and energy of the ^{7}Be ions. A scaled drawing of the experimental setup in Fig. 2 shows the position of the Si detector relative to the Au target foil. The Si detector has concentric ring electrodes on the upstream side and radial sectors on the downstream side allowing the measurement of particles scattering in an angular range of 24°–55°. The S2 Si detector rings begin 11 mm from the center of the detector and end at 35 mm and there are 48 rings with 0.5- mm pitch. Pairs of adjacent rings were electrically combined in the front-end feedthrough to make 24 rings, each effectively 1- mm wide each.

Outside of the scattering chamber, six High-Purity Germanium (HPGe) clover detectors from the Clovershare collaboration measured γ rays in coincidence with the ^{7}Be ions. The detectors were placed around the gold foil, positioned 20 cm away and at 45°, 90°, and 135° from the beam axis. Bismuth Germanate (BGO) shields surrounded the HPGe detectors. Although Compton suppression was not used in this experiment, the BGO shields provided passive shielding from external background γ rays and the BGO shield hevimet collimators provided collimation for the γ rays produced in the experiment.

Signals from both the Si and HPGe detectors were run through preamplifiers into a digital data acquisition system, which had a sampling frequency of 100 MHz. The data were written in list mode onto hard disk using the Pixie-16 system [49]. An event was defined by a hit in a ring of the Si detector with a coincidence timing window of 2 μs, though only events which saw hits in both a ring and a sector were used in the experiment. An example spectrum of the different particles seen in the detector is shown in Fig. 3, with the central peak of the ^{7}Be particles separated from the lower energy contaminants.

The energy and efficiency of the HPGe detectors were calibrated with a 1.468 μCi ^{152}Eu source. The detector array had a total γ-ray efficiency of 1.4% at 500 keV. The energy calibration was also verified by observing γ rays from the Coulomb excitation of ^{197}Au at their appropriate energies. The 67 keV ^{197}Au x ray and 77 keV, 277 keV, and 547 keV γ rays were seen. The energy resolution of our array was 2.8 keV at 1408 keV and was sufficient for our measurement.

III. ANALYSIS

The experimental analysis consisted of three major parts. First, the yield of ^{7}Be γ rays was determined from the Doppler-corrected spectrum using recoil position information from the Si detector. Second, the integrated beam flux was determined by comparing the measured rates of ^{7}Be scatter to Monte Carlo simulations. Finally, by combining this information, the $B(E2)$ transition strength was calculated using the Winther-De Boer Coulomb excitation code [50]. The details of the analysis are presented below.

The direction of the ^{7}Be ions detected in the Si detector was used to correct for the Doppler shift of the γ rays emitted in flight. Random coincidences were eliminated by requiring a tight time coincidence between the Si and Ge detector

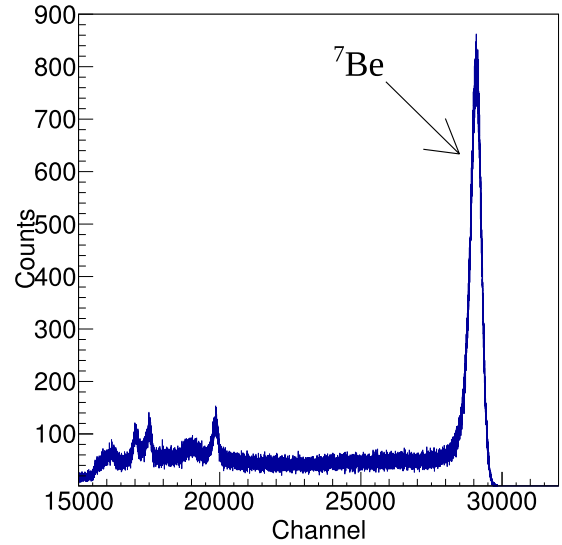

FIG. 3. Shown above is an energy spectrum of particles seen in the 4th ring of our S2 particle detector from the center, corresponding to a nominal angle of 31.8°. The data shown are only from ring events where a corresponding event in a sector of our detector was also seen. The high energy peak pictured is the elastically scattered ^{7}Be while the smaller peaks are various contaminants of our beam that scattered through *TwinSol* at lower energies.

signals. The Doppler-corrected spectrum yielded a peak with a centroid value of 431 keV with a FWHM of 10 keV. This energy corresponds to the $1/2^- \rightarrow 3/2^-$ transition of ^{7}Be and is shown in Fig. 4. We fit our γ-ray peak with a Gaussian function and a linear background, which yielded a total peak area of 30(6) *counts*. The calibrated efficiency of the HPGe array was used to determine our final γ yield.

Determining the ^{7}Be beam flux on the Au target was a necessary step in calculating the $B(E2)$ value. Production of in-flight beams with *TwinSol* typically produces extended spot sizes on target. A LISE++ [51] calculation of the beam transport through *TwinSol* to the Au target showed a fairly uniform beam with a radius on the order of 5 mm. Due to the diffuseness of the beam and the proximity of the target to the Si detector, the rings of the Si detector detected ^{7}Be ions from

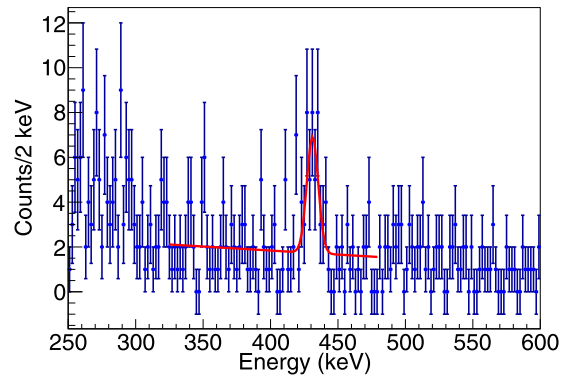

FIG. 4. The total, Doppler-corrected γ-ray spectrum, taken in coincidence with particles seen in the silicon detector, is shown. The spectrum is binned with 2 keV/bin. The γ-ray peak corresponding to the $1/2^- \rightarrow 3/2^-$ transition of ^{7}Be is seen at 431 keV.

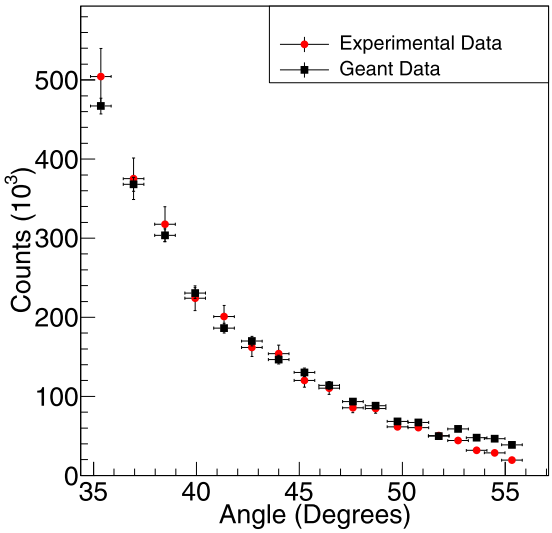

FIG. 5. A plot of ^{7}Be ions measured in the rings of the Si detector (circles) and the Geant4 simulated data (squares).

a range of scattering angles. The Si detector sectors can also show asymmetry in the measured rates if the incident beam is offset. To properly account for these effects, a Geant4 [52–54] simulation was performed to deduce the beam rate on target. Two beam parameters were varied in the simulation: the beam radius and the offset from the beam axis. The angular spread for the incident beam was also considered but we found it had little impact on the simulation. These beam parameters were scanned over a range of values (2 mm-8 mm for the radius and 3 mm-7 mm for the offset) to find the optimal parameters that reproduced the distribution seen in the rings and sectors. A 4 mm beam radius and a 4 mm offset best reproduced the shape of the Si detector ring and sector data. The reproduction of the experimental data seen in the Si detector rings is shown in Fig. 5. The agreement between the Geant4 simulation and the data was good and yielded a beam rate of $8.8(4) \times 10^4$ pps. The uncertainty in the beam rate was estimated by how much the beam parameters can be changed before the shape of the beam exceeded the experimental uncertainties.

Next, the ^{7}Be $B(E2)$ was calculated using a version of the Winther-De Boer Coulomb excitation code modified to perform calculations for electric dipole to hexadecapole transitions based on the semi-classical theory of Coulomb excitation [55]. The Winther-De Boer code calculates differential cross sections as a function of angle given an $E2$ matrix element. The $E2$ matrix element was varied to reproduce the γ-ray yield measured in the experiment. Because the ^{7}Be beam was broad, the different scattering angles and detector geometric efficiencies were accounted for using the Geant4 simulation mentioned above. The ^{7}Be $B(E2; 3/2^- \rightarrow 1/2^-)$ value we obtained is $26(6)\, e^2\,\mathrm{fm}^4$, which includes the statistical and beam rate uncertainties. This value differs from our previous reported preliminary result of $34(8)\, e^2\,\mathrm{fm}^4$ [56] due to the use of a default value of the $E1$ dipole polarizability term in our previous calculation. This default value was initially thought to be negligible but turned out to significantly modify the Coulomb excitation cross section. We have verified that we are able to completely turn off the contribution from the $E1$ polarizability term in our current calculation and have also checked our calculated cross sections by using the same input parameters with the coupled-channels code FRESCO [57] and found the results consistent.

There were a number of systematic uncertainties associated with the measurement. Two important considerations in deducing the $B(E2; 3/2^- \rightarrow 1/2^-)$ transition strength are the influence of second-order processes and the contribution of the $M1$ excitation to the Coulomb excitation cross section. Of the second-order processes, the largest is the virtual $E1$ excitation to the ^{3}He-α breakup channel, the $E1$ dipole polarizability. This effect is known to alter the Coulomb excitation cross section on the order of 10 percent at the energy and angles used on our experiment, based on the estimated dipole polarizability seen in ^{7}Li [58]. This is due to the low-energy threshold for breakup, which is at 1.59 MeV. The total $M1$ excitation contributing to the Coulomb excitation cross section is calculated to be less than 3% for forward angles. Due to these effects, we make a combined estimate for our systematic uncertainty as 13% and 3% for the effect of the $E1$ dipole polarizability and the $M1$ excitation, respectively. This gives a value of $\pm 3\, e^2\,\mathrm{fm}^4$. The uncertainties in our measurement stem primarily from this systematic uncertainty due to $E1$ excitations and to the limited statistics gathered in the experiment.

IV. COMPARSION WITH *AB INITIO* THEORY

To use the present experimental result for the $B(E2; 3/2^- \rightarrow 1/2^-)$ strength in ^{7}Be as a test of *ab initio* theory, we must contend with the convergence limitations described in the introduction. Recall that the mathematical problem to be solved in the *ab initio* nuclear description of the nucleus is well-defined: find the eigenvalues and eigenfunctions of the many-body Schrödinger equation, for A nucleons, which are interacting by a given internucleon interaction. However, this is a formidable computational problem, and the accuracy of the solutions is limited by available computational power. Observables which are sensitive to the long-range physics of the nucleus (the tails of the nuclear wave function), such as $E2$ matrix elements and charge radii, can be particularly challenging to compute.

Only when we have adequately addressed these numerical challenges can we compare the results with experiment, and use this comparison as a meaningful test of the predictive power of *ab initio* nuclear theory. Recall that the fundamental input to the *ab initio* description is the imperfectly-known internucleon interaction entering into the many-body Schrödinger equation.[1]

[1]Since nucleons are not simply point particles, electromagnetic observables calculated from the *ab initio* wave functions also depend upon the electromagnetic current operators for the nucleons [35]. These current operators may need significant corrections from, e.g., meson-exchange currents, going beyond the single-nucleon impulse approximation. Chiral approaches likewise provide a systematic approach to determining the current operators [59].

TABLE I. *Ab initio* GFMC predictions for absolute $B(E2; 3/2^- \rightarrow 1/2^-)$ strengths in ^{7}Li and ^{7}Be. Experimental values are shown for comparison. All values are given in $e^2\text{fm}^4$.

Method	Interaction	^{7}Li	^{7}Be	Reference
GFMC	AV18+IL2	8.09(17)	25.6(3)	[34][a]
	AV18+IL2	8.15(20)	27.5(8)	[34][b]
	AV18+IL7	7.81(45)	22.2(11)	[35]
Experiment		8.3(5)		[31]
			26(6)(3)	Present

[a]Computed using "Type I" trial wave functions and reprojected interactions (AV8′ + IL2′).
[b]Computed using "Type II" trial wave functions and reprojected interactions (AV8′ + IL2′).

We start by noting that the Green's function Monte Carlo (GFMC) approach is able to directly provide calculations of absolute $E2$ strengths, with well-defined statistical uncertainties from the Monte Carlo calculation. Predictions for the absolute $B(E2)$ strengths in ^{7}Li and ^{7}Be, from Refs. [34,35], are shown in Table I, along with the experimental values. These calculations are based on an internucleon interaction with an AV18 two-body part [39] and either an IL2 [40] or IL7 [42] three-body contribution. The calculated values for the $E2$ strength in ^{7}Li are generally consistent with the measured value. There is significantly greater variation among the calculated values for the $E2$ strength in ^{7}Be, with these values lying either just inside or just outside the lower edge of the uncertainty on the present measured value.

However, the GFMC approach is limited in its ability to accommodate state-of-the-art nonlocal chiral EFT interactions [21,60]. There can furthermore be systematic effects in the many-body calculation [21], e.g., from clusterization [9], which may not be accounted for in the statistical uncertainties. It is therefore important to also move forward with comparisons against NCSM results.

The NCSM is based on solving for the nuclear many-body wave functions in a basis of antisymmetrized products (Slater determinants) of single-nucleon wave functions, which are usually taken as harmonic oscillator orbitals. Written in terms of this basis, the Schrödinger equation becomes a matrix eigenproblem. However, calculations can only be done with a finite basis, and the accuracy of results depends on how well the true solution to the Schrödinger equation for the many-body wave function can be approximated in this truncated basis.

In practice, the NCSM basis is truncated by keeping only Slater determinants in which the nucleons have at most some maximum number $N_{\max}$ of oscillator excitations. The numerical accuracy of the solution can, in principle, be made arbitrarily good by increasing $N_{\max}$, but the number of basis states, and thus the dimension of the matrix eigenproblem, grows rapidly with $N_{\max}$ (e.g., reaching $\sim 2.5 \times 10^8$ for the largest calculations for ^{7}Be and ^{7}Li, with $N_{\max} = 12$, shown here) and eventually becomes prohibitive. The accuracy of the calculation also depends sensitively on the oscillator length scale (quoted here as an oscillator frequency $\hbar\omega$) chosen for the basis.

To illustrate the convergence of NCSM results, let us momentarily restrict our attention to one specific internucleon interaction, the Daejeon16 interaction [43]. We carry out NCSM calculations for this interaction, using the code MFDn [61–63], to obtain energies and electromagnetic transition strengths, presented in Fig. 6. (Numerical tabulations of the calculated observables in Fig. 6 are provided in the Supplemental Material [64].)

For instance, for the ground-state energy of ^{7}Be, we can see how the values calculated in truncated bases approach the actual ground state energy of this Schrödinger equation problem by examining Fig. 6(a). At fixed basis size, e.g., the uppermost curve shows calculations for $N_{\max} = 2$, the calculated energy depends upon $\hbar\omega$, but has a variational minimum at some value of $\hbar\omega$. As the basis is enlarged to $N_{\max} = 4$, 6, etc., we obtain the successively lower curves. The approach to a converged result is indicated as the calculated values become independent of $N_{\max}$ (the curves lie atop one another) and independent of $\hbar\omega$ (the curves become flat).

If we were considering $M1$ transitions, then convergence would readily be obtained, as seen in Fig. 6(b) for the strength of the lowest $M1$ transition. We see that the prediction for $B(M1; 3/2^- \rightarrow 1/2^-)$ can be identified to well within 0.1 μ_N^2, even from low-$N_{\max}$ calculations.

However, the calculated $B(E2)$ values, shown in Fig. 6(c), are still steadily changing as the basis size increases, even at $N_{\max} = 12$. There is no clear indication from these truncated calculations as to what the actual solution is for the $E2$ strength in the full, untruncated *ab initio* problem. (There is perhaps at most a hint of a flattening of the curves at the lower end of the $\hbar\omega$ range.) The same general behavior holds for the $B(E2)$ values calculated for ^{7}Be (solid curves) and ^{7}Li (dashed curves), although with different overall scales. In fact, therein lies the essential observation—that the convergence of the two $E2$ values follows a similar pattern, except for scale, and that their ratio may therefore be stable.

For the ratio to be stable with respect to $\hbar\omega$ and $N_{\max}$, the transition strengths entering into the ratio must have the same overall form for their convergence behavior, as functions of $N_{\max}$ and $\hbar\omega$, differing only in an overall normalization factor. This is plausible if the wave functions of the states involved have similar structure, but the convergence behavior of $E2$ observables is in general not well understood (see, e.g., Ref. [65] for a proposed functional form for their convergence in the two-body system), and the degree of convergence of the ratio is for now a matter to be determined empirically.

In NCSM calculations of $E2$ transitions within rotational bands in light nuclei [30,66,67] it has been found that, even though each of the $E2$ transition strengths within the band is not individually converged, the *ratios* of $E2$ strengths within a rotational band already converge to approximately rotational ratios at low $N_{\max}$ (see Fig. 8 of Ref. [30]). We now similarly consider a ratio of $E2$ strengths across analog transitions in mirror nuclei, in Fig. 6(d). Given that the initial and final states in the ^{7}Be $3/2^- \rightarrow 1/2^-$ transition are isobaric analog states to those in the ^{7}Li $3/2^- \rightarrow 1/2^-$ transition, it is not unreasonable that we find similar convergence properties for their wave functions, and thus transition observables, in NCSM calculations. Indeed, it is seen that the calculated ratio

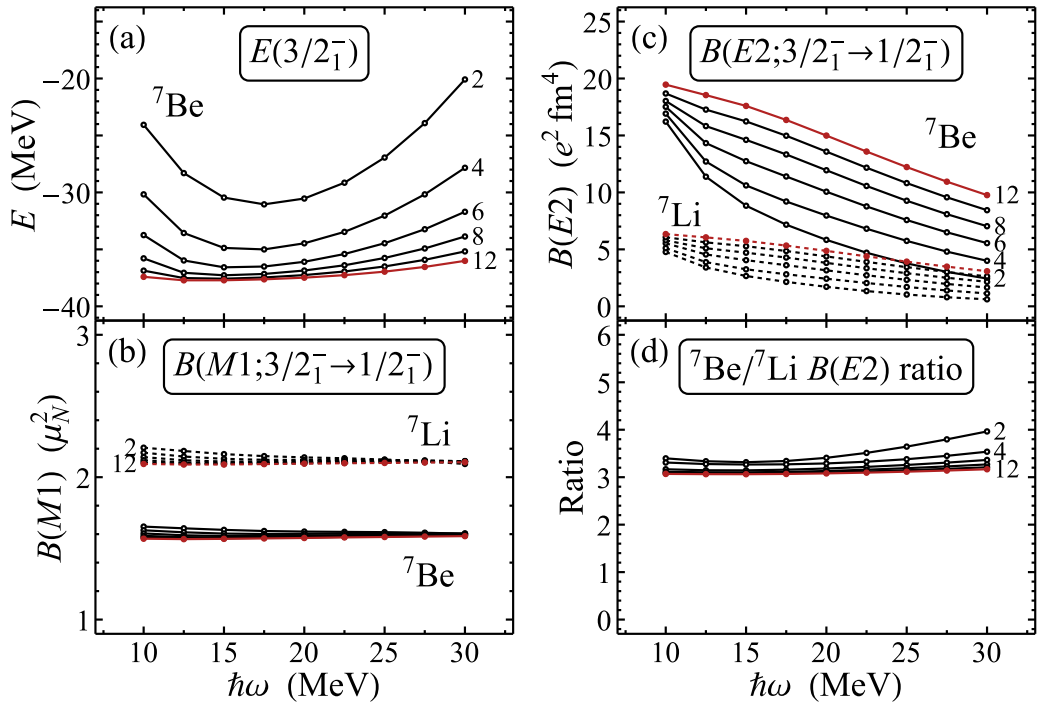

FIG. 6. Convergence of *ab initio* NCSM calculations for ^{7}Li and ^{7}Be, with the Daejeon16 interaction: (a) the $3/2^-$ ground state energy (^{7}Be only), (b) $B(E2;3/2^- \rightarrow 1/2^-)$ for ^{7}Li (dashed curves) and ^{7}Be (solid curves), (c) $B(M1;3/2^- \rightarrow 1/2^-)$ for ^{7}Li (dashed curves) and ^{7}Be (solid curves), and (d) the ratio of $B(E2;3/2^- \rightarrow 1/2^-)$ strengths in ^{7}Li and ^{7}Be. Calculated values are shown as functions of the basis parameter $\hbar\omega$, for $N_{\max} = 2$ to 12 (as labeled).

of $E2$ strengths in ^{7}Be and ^{7}Li converges rapidly, by $N_{\max} \sim 6$, to a value in the range ∼3.0–3.1.

The *ab initio* $E2$ ratio predictions in Fig. 6(d) are based on one particular choice of internucleon interaction, and we must understand the sensitivity of these predictions to the input interaction. Of course, without converged predictions of $E2$ observables in NCSM calculations, it has not been possible to study the sensitivity, to the choice of internucleon interaction, of the predictions for *absolute* $E2$ strengths. However, the ^{7}Be/^{7}Li $B(E2)$ ratio provides a common ground for comparison across different internucleon interactions.

Predictions for the $B(E2)$ ratio from NCSM calculations based on different interactions are compared in Fig. 7.[2] In addition to the Daejeon16 calculations already discussed, we carry out NCSM calculations with the LENPIC N^{2}LO chiral EFT interaction [44]. (Numerical tabulations of the calculated observables as functions of $N_{\max}$ and $\hbar\omega$ are provided in the Supplemental Material [64].) We also compare with ratios extracted from previous NCSM calculations for the JISP16 [41] interaction, taken from Ref. [36], and the classic Entem-Machleidt (EM) N^{3}LO chiral EFT interaction [20], taken from Refs. [37,38].

The Daejeon16 interaction, which we have considered so far above, is obtained from the two-body part of the classic Entem-Machleidt (EM) N^{3}LO chiral EFT interaction with 500 MeV ultraviolet regulator [20], which is then softened via a similarity renormalization group (SRG) transformation and adjusted via a phase-shift equivalent transformation to describe light nuclei, as detailed in Ref. [43]. The JISP16 [41] interaction, in contrast, is derived from nucleon-nucleon scattering data by J-matrix inverse scattering, yielding a two-body interaction which is likewise adjusted via a phase-shift equivalent transformation to describe light nuclei. As an example of a modern chiral EFT interaction, we use the two-body component of the recently-developed LENPIC N^{2}LO interaction with semi-local coordinate space regulator ($R = 1$ fm) [44]. The ratios shown for the EM N^{3}LO interaction

[2]For reference, we detail the basis parameters for the calculations yielding the results in Fig. 7 and record the numerical values for the ratios plotted in this figure: For the JISP16, Daejeon16, and LENPIC interactions, the basis parameter $\hbar\omega$ is chosen at the approximate variational minimum for the ground state energy. The ratios obtained in these NCSM calculations are 3.04 for JISP16 ($N_{\max} = 16$, $\hbar\omega = 20$ MeV; see Tables II and IV of Ref. [36]), 3.06 for Daejeon16 ($N_{\max} = 12$, $\hbar\omega = 12.5$ MeV), and 3.10 for LENPIC N^{2}LO ($N_{\max} = 12$, $\hbar\omega = 27.5$ MeV). For EM N^{3}LO, the ratios are based on $E2$ strengths extracted in Ref. [38] from the wave functions computed in Ref. [37]. These yield a ratio of 3.13 from the NCSM calculations ($N_{\max} = 10$, $\hbar\omega = 20$ MeV) and 2.81 from the NCSMC calculations (which combine this NCSM basis for the $A = 7$ system with an $N_{\max} = 12$ RGM cluster basis). The GFMC ratios are obtained from the $B(E2)$ values already described above in Table I, while the uncertainties shown on the ratios are obtained by combining the statistical uncertainties on the individual calculated $B(E2)$ values in quadruature: the resulting ratios are 3.16(8), 3.37(13), and 2.8(2), corresponding to the first three rows in Table I, respectively.

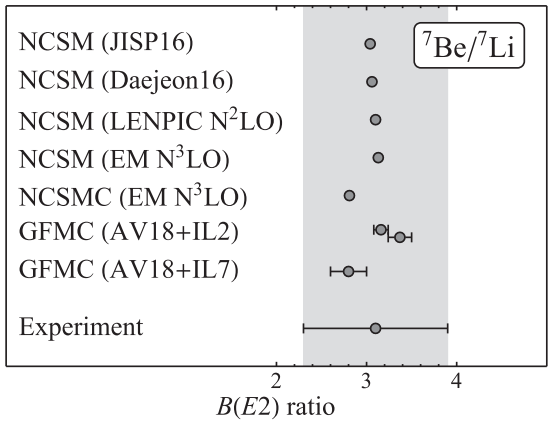

FIG. 7. *Ab initio* predictions for the ratio of the $B(E2; 3/2^- \rightarrow 1/2^-)$ strength in ^{7}Be to that in ^{7}Li, obtained by various many-body solution methods and for various internucleon interactions (see text). The experimental ratio is shown for comparison with 1σ uncertainties. Further details of the calculations may be found in the text (see also footnote 2).

are based on the two-body component of this interaction [20], softened via a similarity renormalization group (SRG) transformation to a resolution scale of $\Lambda = 2.15\,\mathrm{fm}^{-1}$.

The notable point in Fig. 7 is the remarkable consistency of the predictions for the $B(E2)$ ratio from the *ab initio* NCSM calculations, essentially independent of the choice of interaction. We may compare these with an experimental ratio of 3.1(8), obtained based on the experimental values in Table I (the uncertainties on the ^{7}Be and ^{7}Li $E2$ strengths have simply been treated as uncorrelated and combined in quadrature). The *ab initio* NCSM predictions for the ratio are all within the experimental uncertainty range and agree with the measured result.

The $B(E2)$ ratio furthermore provides a means of comparing predictions, not just across interactions, but across different many-body solution methods, as also shown in Fig. 7. In such a comparison, we should keep in mind that convergence behaviors differ across many-body methods, so the convergence of the calculated ratio must ultimately be reassessed for each method.

The $E2$ ratios obtained using the different sets of GFMC calculations from Table I scatter signficiantly more than the ratios obtained from the NCSM calculations, as shown in Fig. 7. However, they are approximately consistent with the NCSM values to within the statistical uncertainties.

By explicitly including cluster degrees of freedom into the NCSM basis, the no-core shell model with continuum (NCSMC) approach [27] attempts to attain more rapidly convergent calculations. NCSMC calculations for ^{7}Li and ^{7}Be are presented in Ref. [37], for the EM N^{3}LO interaction. These combine an $A = 7$ (^{7}Li or ^{7}Be) NCSM basis at $N_{\max} = 10$ and $\hbar\omega = 20$ MeV with microscopic cluster states (involving ^{4}He and ^{3}H or ^{3}He clusters) at $N_{\max} = 12$. The $B(E2)$ values obtained from these NCSMC wave functions are $7.12\,e^2\,\mathrm{fm}^4$ for ^{7}Li and $20.02\,e^2\,\mathrm{fm}^4$ for ^{7}Be [38], comparable to experiment (the corresponding ratio is shown in Fig. 7). For comparison, NCSM calculations with the same interaction yield $B(E2)$ strengths ranging from $2.66\,e^2\,\mathrm{fm}^4$ at $N_{\max} = 6$ to $3.486\,e^2\,\mathrm{fm}^4$ at $N_{\max} = 10$ for ^{7}Li, or $8.45\,e^2\,\mathrm{fm}^4$ at $N_{\max} = 6$ to $10.901\,e^2\,\mathrm{fm}^4$ at $N_{\max} = 10$ for ^{7}Be [38].

In summary, *ab initio* predictions obtained using a variety of realistic internucleon interactions and different many-body solution methods give remarkably robust and consistent predictions for the $B(E2)$ ratio between the mirror transitions in ^{7}Be and ^{7}Li (Fig. 7), with a spread of only $\sim$2% in the NCSM results, or $\lesssim$20% if the GFMC and NCSMC calculations are considered as well. The current experimental results (Table I) for the strengths in ^{7}Be and ^{7}Li are consistent with the calculated NCSM GFMC results, within the one-sigma uncertainty range on the experimental value. It should be noted that the experimental value we have used for the $B(E2)$ strength in ^{7}Li is the evaluated value [31], but conflicting results may be found among the various Coulomb excitation measurements and analyses [58,68–75]. More precise experimental values, for both mirror isotopes, would provide a more stringent test of the *ab initio* theory.

V. SUMMARY AND OUTLOOK

We have performed a radioactive beam Coulomb excitation experiment to measure the $B(E2; 3/2^- \rightarrow 1/2^-)$ transition strength in ^{7}Be for the first time, with the aim of testing the ability of *ab initio* theory to provide accurate predictions of electromagnetic observables. Although $E2$ observables can present a computational challenge to the *ab initio* many-body solution methods, due to their sensitivity to the long-range components of the wave functions, we have found that the ratios of $E2$ strengths for isospin mirror transitions are robustly converged in NCSM calculations. The calculated ratios are remarkably consistent across internucleon interactions and many-body solution methods.

We combine our measured ^{7}Be transition strength $[B(E2; 3/2^- \rightarrow 1/2^-) = 26(6)(3)\,e^2\,\mathrm{fm}^4]$ with the known ^{7}Li transition strength to obtain an experimental ratio of $B(E2)_{^7\mathrm{Be}}/B(E2)_{^7\mathrm{Li}} = 3.1(8)$. This is generally consistent, within uncertainty, with the *ab initio* predictions, which cluster around $\sim$3.1, well within the experimental one-sigma uncertainty range.

To provide a more comprehensive set of precision electromagnetic tests of *ab initio* theory for light nuclei, the $B(E2)$ ratio should be investigated for additional mirror transitions (and possibly nonmirror transitions), such as in the $A = 8$ isobars ^{8}Li and ^{8}B. A previous Coulomb excitation measurement has yielded the $E2$ transition strength in ^{8}Li $[B(E2; 2^+ \rightarrow 1^+) = 55(11)\ e^2\,\mathrm{fm}^4]$ [48], but the $E2$ transitions strength in ^{8}B is currently unknown. While so far only unconverged NCSM calculations of the ^{8}Li $B(E2; 2^+ \rightarrow 1^+)$ transition strength have been discussed [76], we expect that the convergence limitations in the NCSM calculations can again be overcome by considering the ratio with the ^{8}B mirror transition strength.

New data on electromagnetic observables for these and other light nuclei would give tighter constraints on the various *ab initio* descriptions that are now available and either validate or challenge our understanding of the microscopic origins of nuclear structure in this region. Such tests of nuclear theory

will both validate and contribute to the development of a higher degree of predictive power for *ab initio* approaches. These approaches promise to have significant implications not only for nuclear structure, but for nuclear interactions and nuclear astrophysics as well, such as in the calculation of low-energy S factors [37,77,78].

ACKNOWLEDGMENTS

We thank S. Quaglioni and collaborators for sharing their NCSMC results for the $B(E2; 3/2^- \rightarrow 1/2^-)$ for ^{7}Li and ^{7}Be, P. Navratil and S. Quaglioni for comments on the manuscript, and K. Nollett for pointing us toward the results of S. Pastore. We thank A. Moro for performing coupled-channels calculations for our experiment. We also thank X. Li and J. Riggins for their help during data collection. We also acknowledge the Clovershare collaboration for the use of the HPGe Clover detectors at the NSL at the University of Notre Dame. This work was supported by the US National Science Foundation under Grants No. PHY 17-13857, No. PHY 14-01343, and No. PHY 14-30152 and the US Department of Energy under Grant No. DE-FG02-95ER-40934. TRIUMF receives federal funding via a contribution agreement with the National Research Council of Canada. This research used computational resources of the National Energy Research Scientific Computing Center (NERSC), which is a DOE Office of Science User Facility (Contract DE-AC02-05CH11231).

[1] A. Bohr and B. R. Mottelson, *Nuclear Structure* (World Scientific, Singapore, 1998), Vol. 1.
[2] P. J. Twin, B. M. Nyakó, A. H. Nelson, J. Simpson, M. A. Bentley, H. W. Cranmer-Gordon, P. D. Forsyth, D. Howe, A. R. Mokhtar, J. D. Morrison, J. F. Sharpey-Schafer, and G. Sletten, Phys. Rev. Lett. **57**, 811 (1986).
[3] H. Gao, Int. J. Mod. Phys. E **12**, 1 (2003).
[4] C. E. Hyde-Wright and K. de Jager, Annu. Rev. Nucl. Part. Sci. **54**, 217 (2004).
[5] J. Aubert, G. Bassompierre, K. Becks, C. Best, E. Böhm, X. de Bouard, F. Brasse, C. Broll, S. Brown, J. Carr *et al.*, Phys. Lett. B **123**, 275 (1983).
[6] J. Gomez, R. G. Arnold, P. E. Bosted, C. C. Chang, A. T. Katramatou, G. G. Petratos, A. A. Rahbar, S. E. Rock, A. F. Sill, Z. M. Szalata, A. Bodek, N. Giokaris, D. J. Sherden, B. A. Mecking, and R. M. Lombard-Nelsen, Phys. Rev. D **49**, 4348 (1994).
[7] R. Pohl, R. Gilman, G. A. Miller, and K. Pachucki, Annu. Rev. Nucl. Part. Sci. **63**, 175 (2013).
[8] E. A. McCutchan, C. J. Lister, R. B. Wiringa, S. C. Pieper, D. Seweryniak, J. P. Greene, M. P. Carpenter, C. J. Chiara, R. V. F. Janssens, T. L. Khoo, T. Lauritsen, I. Stefanescu, and S. Zhu, Phys. Rev. Lett. **103**, 192501 (2009).
[9] E. A. McCutchan, C. J. Lister, S. C. Pieper, R. B. Wiringa, D. Seweryniak, J. P. Greene, P. F. Bertone, M. P. Carpenter, C. J. Chiara, G. Gürdal, C. R. Hoffman, R. V. F. Janssens, T. L. Khoo, T. Lauritsen, and S. Zhu, Phys. Rev. C **86**, 014312 (2012).
[10] C. J. Lister and E. A. McCutchan, Nucl. Data Sheets **120**, 84 (2014).
[11] S. A. Kuvin, A. H. Wuosmaa, C. J. Lister, M. L. Avila, C. R. Hoffman, B. P. Kay, D. G. McNeel, C. Morse, E. A. McCutchan, D. Santiago-Gonzalez, and J. R. Winkelbauer, Phys. Rev. C **96**, 041301 (2017).
[12] P. Navrátil, J. P. Vary, and B. R. Barrett, Phys. Rev. Lett. **84**, 5728 (2000).
[13] S. C. Pieper, R. B. Wiringa, and J. Carlson, Phys. Rev. C **70**, 054325 (2004).
[14] T. Neff and H. Feldmeier, Nucl. Phys. A **738**, 357 (2004).
[15] G. Hagen, D. J. Dean, M. Hjorth-Jensen, T. Papenbrock, and A. Schwenk, Phys. Rev. C **76**, 044305 (2007).
[16] E. Epelbaum, H. Krebs, D. Lee, and Ulf-G. Meißner, Phys. Rev. Lett. **106**, 192501 (2011).
[17] S. Bacca, N. Barnea, and A. Schwenk, Phys. Rev. C **86**, 034321 (2012).
[18] N. Shimizu, T. Abe, Y. Tsunoda, Y. Utsuno, T. Yoshida, T. Mizusaki, M. Honma, and T. Otsuka, Prog. Exp. Theor. Phys. **2012**, 01A205 (2012).
[19] E. Epelbaum, H.-W. Hammer, and U.-G. Meißner, Rev. Mod. Phys. **81**, 1773 (2009).
[20] D. R. Entem and R. Machleidt, Phys. Rev. C **68**, 041001 (2003).
[21] J. Carlson, S. Gandolfi, F. Pederiva, S. C. Pieper, R. Schiavilla, K. E. Schmidt, and R. B. Wiringa, Rev. Mod. Phys. **87**, 1067 (2015).
[22] P. Navrátil, S. Quaglioni, I. Stetcu, and B. R. Barrett, J. Phys. G **36**, 083101 (2009).
[23] B. R. Barrett, P. Navrátil, and J. P. Vary, Prog. Part. Nucl. Phys. **69**, 131 (2013).
[24] R. Roth and P. Navrátil, Phys. Rev. Lett. **99**, 092501 (2007).
[25] S. Quaglioni and P. Navrátil, Phys. Rev. C **79**, 044606 (2009).
[26] T. Dytrych, K. D. Launey, J. P. Draayer, P. Maris, J. P. Vary, E. Saule, U. Catalyurek, M. Sosonkina, D. Langr, and M. A. Caprio, Phys. Rev. Lett. **111**, 252501 (2013).
[27] C. Romero-Redondo, S. Quaglioni, P. Navrátil, and G. Hupin, Phys. Rev. Lett. **117**, 222501 (2016).
[28] A. E. McCoy, M. A. Caprio, and T. Dytrych, Ann. Acad. Rom. Sci. Ser. Chem. Phys. Sci. **3**, 17 (2018).
[29] P. Maris and J. P. Vary, Int. J. Mod. Phys. E **22**, 1330016 (2013).
[30] M. A. Caprio, P. Maris, J. P. Vary, and R. Smith, Int. J. Mod. Phys. E **24**, 1541002 (2015).
[31] D. R. Tilley, C. M. Cheves, J. L. Godwin, G. M. Hale, H. M. Hofmann, J. H. Kelley, C. G. Sheu, and H. R. Weller, Nucl. Phys. A **708**, 3 (2002).
[32] D. S. P. Bunbury, S. Devons, G. Manning, and J. H. Towle, Proc. Phys. Soc. A **69**, 165 (1956).
[33] P. Paul, J. B. Thomas, and S. S. Hanna, Phys. Rev. **147**, 774 (1966).
[34] M. Pervin, S. C. Pieper, and R. B. Wiringa, Phys. Rev. C **76**, 064319 (2007).
[35] S. Pastore, S. C. Pieper, R. Schiavilla, and R. B. Wiringa, Phys. Rev. C **87**, 035503 (2013).
[36] T. Heng, J. P. Vary, and P. Maris, Phys. Rev. C **95**, 014306 (2017).
[37] J. Dohet-Eraly, P. Navrátil, S. Quaglioni, W. Horiuchi, G. Hupin, and F. Raimondi, Phys. Lett. B **757**, 430 (2016).
[38] S. Quaglioni (private communication).

[39] R. B. Wiringa, V. G. J. Stoks, and R. Schiavilla, Phys. Rev. C **51**, 38 (1995).

[40] S. C. Pieper, V. R. Pandharipande, R. B. Wiringa, and J. Carlson, Phys. Rev. C **64**, 014001 (2001).

[41] A. M. Shirokov, J. P. Vary, A. I. Mazur, and T. A. Weber, Phys. Lett. B **644**, 33 (2007).

[42] S. C. Pieper, in *New Facet Of Three Nucleon Force 50 Years Of Fujita Miyazawa Three Nucleon Force (FM50): Proceedings of the International Symposium on New Facet of Three Nucleon Force*, edited by H. Sakai, K. Sekiguchi, and B. F. Gibson, AIP Conf. Proc. No. 1011 (AIP, New York, 2008), p. 143.

[43] A. M. Shirokov, I. J. Shin, Y. Kim, M. Sosonkina, P. Maris, and J. P. Vary, Phys. Lett. B **761**, 87 (2016).

[44] S. Binder, A. Calci, E. Epelbaum, R. J. Furnstahl, J. Golak, K. Hebeler, H. Kamada, H. Krebs, J. Langhammer, S. Liebig, P. Maris, Ulf-G. Meißner, D. Minossi, A. Nogga, H. Potter, R. Roth, R. Skibiński, K. Topolnicki, J. P. Vary, and H. Witała (LENPIC Collaboration), Phys. Rev. C **93**, 044002 (2016).

[45] F. D. Becchetti, M. Y. Lee, T. W. O'Donnell, D. A. Roberts, J. J. Kolata, L. O. Lamm, G. Rogachev, V. Guimarães, P. A. DeYoung, and S. Vincent, Nucl. Instrum. Methods A **505**, 377 (2003).

[46] S. Vincent, A. Aprahamian, J. Kolata, L. Lamm, V. Guimarâes, R. de Haan, D. Peterson, P. Santi, A. Teymurazyan, F. Becchetti, T. O'Donnell, M. Lee, D. Roberts, J. Zimmerman, and J. Brown, Nucl. Instrum. Methods Phys. Res. Sec. A: Accel., Spectrom., Detect. Assoc. Equip. **491**, 426 (2002).

[47] H. Amro, F. Becchetti, H. Jiang, M. Ojaruega, J. Kolata, B. Skorodumov, G. Peaslee, P. Young, D. Denby, and J. Hinnefeld, Nucl. Instrum. Methods Phys. Res. Sec. A: Accel., Spectrom., Detect. Assoc. Equip. **579**, 31 (2007).

[48] J. A. Brown, F. D. Becchetti, J. W. Janecke, K. Ashktorab, D. A. Roberts, J. J. Kolata, R. J. Smith, K. Lamkin, and R. E. Warner, Phys. Rev. Lett. **66**, 2452 (1991).

[49] S. Lipschutz, R. Zegers, J. Hill, S. Liddick, S. Noji, C. Prokop, M. Scott, M. Solt, C. Sullivan, and J. Tompkins, Nucl. Instrum. Methods A **815**, 1 (2016).

[50] A. Winther and J. de Boer, *A Computer Program for Multiple Coulomb Excitation*, Tech. Rep. (California Institute of Technology and Rutgers, The State University, 1965).

[51] O. B. Tarasov and D. Bazin, Nucl. Instrum. Methods B **266**, 4657 (2008).

[52] S. Agostinelli, J. Allison, K. Amako, J. Apostolakis, H. Araujo, P. Arce, M. Asai, D. Axen, S. Banerjee, G. Barrand *et al.*, Nucl. Instrum. Methods A **506**, 250 (2002).

[53] J. Allison, K. Amako, J. Apostolakis, H. Araujo, P. A. Dubois, M. Asai, G. Barrand, R. Capra, S. Chauvie, R. Chytracek *et al.*, IEEE Trans. Nucl. Sci. **53**, 270 (2006).

[54] J. Allison, K. Amako, J. Apostolakis, P. Arce, M. Asai, T. Aso, E. Bagli, A. Bagulya, S. Banerjee, G. Barrand *et al.*, Nucl. Instrum. Meth. A **835**, 186 (2016).

[55] K. Alder, A. Bohr, T. Huus, B. Mottelson, and A. Winther, Rev. Mod. Phys. **28**, 432 (1956).

[56] T. Ahn, S. Henderson, A. Simon, W. Tan, J. Allen, D. W. Bardayan, B. Frentz, J. J. Kolata, X. Li, P. O'Malley, M. R. Hall, C. Reingold, J. Riggins, S. Strauss, and R. Torres-Isea, in *Proceeding of the 4th International Workshop on "State of the Art in Nuclear Cluster Physics" (SOTANCP4)*, edited by M. Barbui, C. M. Folden III, V. Z. Goldberg, and G. V. Rogachev, AIP Conf. Proc. No. 2038 (AIP, New York, 2018), p. 020005.

[57] I. J. Thompson, Comput. Phys. Rep. **7**, 167 (1988).

[58] O. Häusser, A. McDonald, T. Alexander, A. Ferguson, and R. Warner, Nucl. Phys. A **212**, 613 (1973).

[59] T.-S. Park, D.-P. Min, and M. Rho, Nucl. Phys. A **596**, 515 (1996).

[60] M. Piarulli, L. Girlanda, R. Schiavilla, A. Kievsky, A. Lovato, L. E. Marcucci, S. C. Pieper, M. Viviani, and R. B. Wiringa, Phys. Rev. C **94**, 054007 (2016).

[61] P. Maris, M. Sosonkina, J. P. Vary, E. Ng, and C. Yang, Procedia Comput. Sci. **1**, 97 (2010).

[62] H. M. Aktulga, C. Yang, E. G. Ng, P. Maris, and J. P. Vary, Concurrency Computat.: Pract. Exper. **26**, 2631 (2013).

[63] M. Shao, H. M. Aktulga, C. Yang, E. G. Ng, P. Maris, and J. P. Vary, Comput. Phys. Commun. **222**, 1 (2018).

[64] See Supplemental Material at http://link.aps.org/supplemental/10.1103/PhysRevC.99.064320 for numerical tabulations of observables from the NCSM calculations, for the Daejeon16 and LENPIC interactions.

[65] D. Odell, T. Papenbrock, and L. Platter, Phys. Rev. C **93**, 044331 (2016).

[66] M. A. Caprio, P. Maris, and J. P. Vary, Phys. Lett. B **719**, 179 (2013).

[67] P. Maris, M. A. Caprio, and J. P. Vary, Phys. Rev. C **91**, 014310 (2015).

[68] O. Häusser, A. McDonald, T. Alexander, A. Ferguson, and R. Warner, Phys. Lett. B **38**, 75 (1972).

[69] A. Bamberger, G. Jansen, B. Povh, D. Schwalm, and U. Smilansky, Nucl. Phys. A **194**, 193 (1972).

[70] W. Vermeer, M. Esat, M. Fewell, R. Spear, A. Baxter, and S. Burnett, Phys. Lett. B **138**, 365 (1984).

[71] W. Vermeer, A. Baxter, S. Burnett, M. Esat, M. Fewell, and R. Spear, Aust. J. Phys. **37**, 273 (1984).

[72] A. Weller, P. Egelhof, R. Čaplar, O. Karban, D. Krämer, K.-H. Möbius, Z. Moroz, K. Rusek, E. Steffens, G. Tungate, K. Blatt, I. Koenig, and D. Fick, Phys. Rev. Lett. **55**, 480 (1985).

[73] F. Barker, Y. Kondo, and R. Spear, Aust. J. Phys. **42**, 597 (1989).

[74] W. Vermeer, R. Spear, and F. Barker, Nucl. Phys. A **500**, 212 (1989).

[75] H.-G. Voelk and D. Fick, Nucl. Phys. A **530**, 475 (1991).

[76] P. Maris, J. P. Vary, and P. Navrátil, Phys. Rev. C **87**, 014327 (2013).

[77] K. M. Nollett, Phys. Rev. C **63**, 054002 (2001).

[78] T. Neff, Phys. Rev. Lett. **106**, 042502 (2011).